Desalination and Water Treatment
www.deswater.com
doi: 10.5004/dwt.2020.25766

201 (2020) 313–322
October

Oxidation of pesticide (Coragen) using triple oxide coated titanium electrodes and nano hydroxyapatite as a sorbent

Ramya Thangamani[a], Karthikeyan Velayutham[b], Mariselvam Ammasi Krishnan[b], Anuradha Dhanasekaran[c], Subramaniyan Sivanesan[b,*]

[a]*Environmental Engineering Laboratory, Department of Environmental Sciences, Bharathiar University, Coimbatore – 641046, India, Tel. +91-9840411566; email: rtramya1@gmail.com (R. Thangamani)*
[b]*Department of Applied Science & Technology, Alagappa College of Technology, Anna University, Chennai – 600025, India, Tel. +91-44-22359166; emails: sivanesh1963@gmail.com (S. Sivanesan), karthikeyandv@gmail.com (K. Velayutham), mariselvamak@gmail.com (M.A. Krishnan)*
[c]*Department of Biotechnology, Anna University, Chennai – 600025, India, Tel. +91-44 -22358384; email: anushivan@gmail.com (A. Dhanasekaran)*

Received 24 December 2018; Accepted 24 February 2020

ABSTRACT

The study mainly demonstrates the oxidation of pesticide (coragen) using triple oxide-coated titanium electrodes where *n* hap is used as a sorbent. The main advantage of this electrode is that it consumes minimum energy, takes less processing time, and produces a high amount of pesticide mineralization. In wastewater treatment, the electrooxidation process in organic effluents using boron doped diamond electrode and Pt consumption of energy was very high but at the same time, the consumption of triple oxide-coated titanium electrode energy was very low whereas the mineralization of effluent was very high. Nano hydroxyapatite is a low-cost nontoxic adsorbent which adsorbs the bromide ions present in the coragen during electrolysis. The efficiency of the electrolysis process was analyzed through analytical parameters such as COD, Cl2, and Br. According to the study results, the mineralization of chemical oxygen demand, chloride, and bromide were 79%, 77%, and 67% respectively. The complete mineralization was verified using gas chromatography-mass spectrometry and Fourier transform infrared spectroscopy analysis results.

Keywords: Tripleoxide coated titanium electrode; *n* hap; Ryanodine; Chlorantrianiliprole; Bromide

1. Introduction

Highly toxic substances like insecticides enter non-target organisms including human beings through the food chain life cycle. Due to its molecular structure and stable internal chemical bonding, the majority of the insecticides are non-biodegradable [1]. Pesticides are normally classified into different chemical classes on the basis of their biological activities that cause adverse effects in organisms [2]. Coragen is a new class of pesticide that contains chlorantrianiliprole. Coragen is widely applied on apples to prevent it from getting infected by codling moth (*Cydia pomonella*), apple fruit moth (*Argyresthia conjugella*), and their free leaf-living larvae [3]. Coragen, as a pesticide, affects the flow of calcium ions which are controlled by ryanodine. These receptors play a major role in the excitation and contraction of muscles, secretion of hormones, and neurotransmission activities. These receptors are highly affected by coragen since it belongs to anthranilic diamide class of insecticides [4]. Saltacor and coragen, the two insecticidal perpetrates that contain chlorantraniliprole, are promoted on a large scale now a days [5]. Coragen contains hydrophobic molecules

* Corresponding author.

that bind extensively to biological membranes, especially phospholipid bi-layers, and damage membranes by inducing lipid peroxidation [6–8]. Further, it produces long-term ill effects in marine organisms. The above discussed environmental ill-effects of coragen raise concerns about addressing the pollution it causes. Various technologies and processes such as hydrogen peroxide extraction, UV, ultrasonic radiation, and biodegradation have been proposed for coragen treatment. However, these methods are deemed to be unsuitable to treat highly-concentrated industrial effluents. As a result, ecofriendly methods like the electrochemical treatment process have become one of the prominent areas of research in recent years for wastewater treatment process [9,10]. During the oxidation process, the organic substances which are present in wastewater can be oxidized in two common ways such as direct oxidation and indirect oxidation. Direct oxidation occurs at the anode surface and produces H_2O and CO_2. Indirect oxidation occurs in the presence of strong oxidants such as chlorine, hypochlorite, peroxydisulfate, and ozone to finally produce H_2O and CO_2.

1.1. Electro-oxidation

The mechanism of electrochemical oxidation of wastewater is a complex phenomenon that involves the coupling of electron transfer reaction with a dissociates chemisorption step. In general, two different processes occur at the anode; one is the anode with high electro-catalytic activity, where oxidation occurs at the electrode surface (direct electrolysis) whereas, in metal oxide electrode, the oxidation occurs via a surface mediator on an anodic surface where they are generated continuously (indirect electrolysis). In direct electrolysis, the rate of oxidation depends upon electrode activity, the diffusion rate of pollutants, and current density. On the other hand, temperature, pH, and diffusion rate of the generated oxidants determine the rate of oxidation in indirect electrolysis. In indirect electro-oxidation, the chloride salts of sodium or potassium are added to the wastewater for better conductivity and generation of hypochlorite ions.

The reactions of anodic oxidation of chloride ions that produce chlorine are given below:

$$2Cl^- \rightarrow Cl_2 + 2e^- \quad (1)$$

The liberated chlorine forms the hypochlorous acid

$$Cl_2 + H_2O \rightarrow H^+ + Cl^- + HOCl \quad (2)$$

and further gets dissociated to yield hypochlorite ion

$$HOCl \rightarrow 3H^+ + OCl^- \quad (3)$$

The OCl^- acts as the main oxidizing agent in the wastewater treatment process.

The generated hypochlorite ions act as the main oxidizing agent in the degradation of pollutants. The direct electrooxidation rate of degrading the organic pollutants mainly depends on the anode surface and the applied power density. The anodic reactions are given below. H_2 is ejected at anode surface to produce adsorbed hydroxyl radicals according to the following reaction:

$$MO_x + H_2O \rightarrow MO_x(OH) + H^+ + e^- \quad (4)$$

The adsorbed hydroxyl radicals interact with oxygen which is already present in the oxide-coated anode. The transition of oxygen from adsorbed hydroxyl radicals produces higher oxide MO_x^{+1}.

$$MO_x(^{\bullet}OH) \rightarrow MO_x^{+1} + H^+ + e^- \quad (5)$$

Active oxygen is normally present in two states on anode surface that is, either as hydroxyl radicals or oxygen in the lattice. In the absence of any oxidizable organics, the 'active oxygen' produces dioxygen as per the following reactions:

$$MO_x(OH) \rightarrow MO_x + \tfrac{1}{2}O_2 + H^+ + e^- \quad (6)$$

$$MO_x^{+1} \rightarrow MO_x + \tfrac{1}{2}O_2 \quad (7)$$

When using sodium chloride as the supporting electrolyte, the chloride ion reacts with hydroxyl radicals to form adsorbed hypochlorite radicals for which the reactions are given below:

$$MO_x(^{\bullet}OH) + Cl^- \rightarrow MO_x + (^{\bullet}Cl) + H^+ + 2e^- \quad (8)$$

The adsorbed hypochlorite radicals may interact with oxygen present in the surface anode to form adsorbed hypochlorite radicals according to the following reactions:

$$MO_x(^{\bullet}OC) + Cl^- \rightarrow MO_x^{+1} + Cl_2 + e^- \quad (9)$$

$$MO_x(^{\bullet}OCl) + Cl^- \rightarrow MO_x + \tfrac{1}{2}O_2 + \tfrac{1}{2}Cl_2 + e^- \quad (10)$$

In the presence of oxidizable organics, the physisorbed active oxygen' ($^{\bullet}OH$) should completely combust the organics so that the chemisorption participates in the formation of selective oxidation products (27) according to the following reactions:

$$\tfrac{1}{2}R + MO_x(^{\bullet}OH) \rightarrow \tfrac{1}{2}ROO + H^+ + e^- MO_x \quad (11)$$

$$R + MO_x^{+1} \rightarrow RO + MO_x \quad (12)$$

This study focused on studying the degradation rate of coragen-contaminated wastewater using triple oxide-coated titanium anodes and sorbent nano-hydroxyapatite. The efficiency of electrocatalytic oxidation was assessed through analytical parameters such as chemical oxygen demand (COD), chloride, and bromide. The total degradation of coragen was strongly proved through gas chromatography–mass spectrum and Fourier transform infrared (FTIR) spectroscopy.

2. Materials and methods

2.1. Electrode materials

Titanium tantalum products which provide triple oxide-coated titanium electrodes, with a coating thickness of 6mm, were chosen for the study. The monopolar connection was used in this study. The triple oxide-coated titanium electrode acts as anode whereas the other triple oxide coated electrode acts as a cathode. The coating consists of triple oxide coated titanium electrodes namely Pt, Ir, and Ta with 20, 20, and 10 g/m^2. The triple oxide-coated electrodes have excellent specific electrolytic properties. These electrodes are active in different types of atmospheric conditions including high and low pH, high concentration of Cl_2, and high temperature. Triple oxide-coated titanium electrodes with a dimension of 10 mm × 10 mm × 2.5 mm were used in the study. The hydrothermal method was followed to prepare nano-hydroxyapatite whereas the morphology, functional groups, and the surface area of *n* hap were identified using scanning electron microscopey (SEM), FTIR, and X-ray diffraction (XRD) instruments.

2.2. Analytical methods

A sample container of 250 mL volume was placed on a magnetic stirrer. The concentration of coragen was 1,000 ppm whereas the effluent volume taken was 200 mL with 2.5 mg L^{-1} NaCl concentration. To change the pHs of the effluent, 0.1 NaCl, 0.1 HCl solution, and triple oxide-coated electrode were placed on the top of the sample container with an inter-electrode gap of 2 cm. The surface area of the triple oxide-coated electrode was 617 cm^2. Rectifier DC power supply was connected to supply electric current during electrolysis. The DC rectifier was equipped with a digital ammeter and voltmeter which were linked to a stabilized electric power. Particular time interval-treated effluents were also collected simultaneously. The effluent was well mixed by magnetic stirrer (Fig. 1).

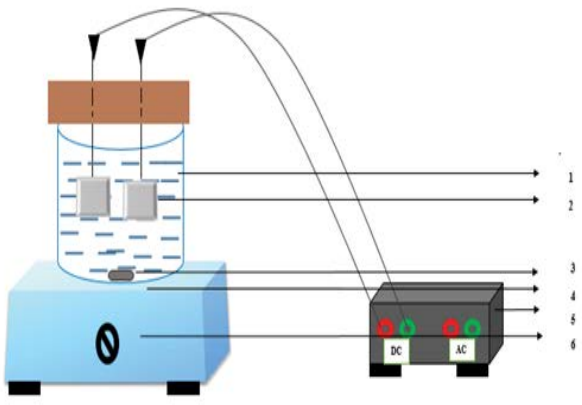

1. Coragen Effluent, 2. Triple oxide coated titanium electrodes, 3. Magnet, 4. Stirrer, 5. Rectifier, 6. Stirrer speed controller

Fig. 1. Schematic representation of the EOP experimental setup.

2.3. Parameters

The open reflex method was used to analyze the COD according to the standard methods (5220 A) (APHA 1995) [11]. Chloride was estimated as per Mohr's method (4500 B-Cl; Argentometric method) and bromide was estimated by the colorimetric method (APHA 4500) using a spectrophotometer at 610 nm.

2.4. Characterization of nano-hydroxyapatite

The (SEM, Hitachi-S4800, 16-1, Higashiueno 2-chome, Taito-ku, Tokyo, 110-0015 Japan) was used to analyze the external features of the *n* hap whereas FTIR (Perkin Elmer, USA) was used to study the functional bonds of *n* hap. The powdered form of *n* hap was recorded with FTIR spectra. X'PERT PRO (The Netherlands) PAN analytical X-ray diffractometer was used to analyze the XRD (Figs. 2–4).

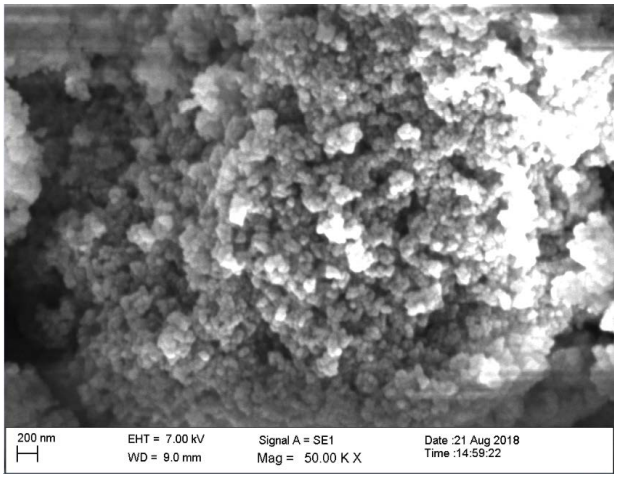

Fig. 2. SEM image of hydroxyapatite.

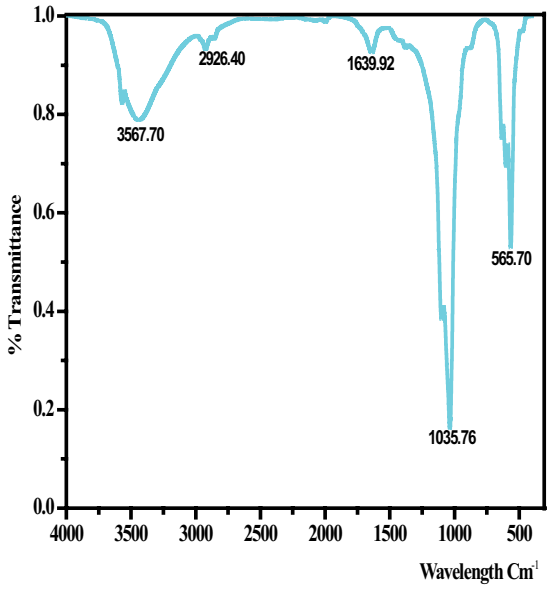

Fig. 3. FTIR image of hydroxyapatite.

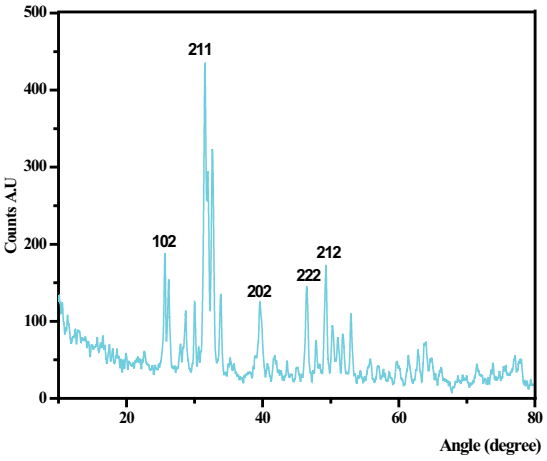

Fig. 4. XRD image of hydroxyapatite.

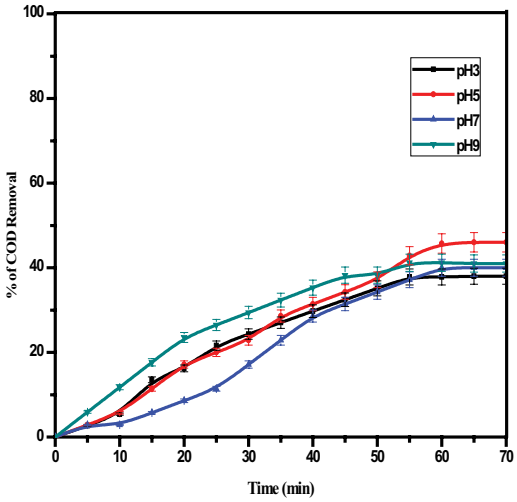

Fig. 5. Various pH on COD.

3. Result and discussion

3.1. Various pHs on COD

In the electrolysis of wastewater, pH is one of the primary key parameters. The total mineralization of coragen during electrolysis using triple oxide-coated titanium electrodes was tested by changing the pH from 3 to 9. During electrolysis, triple oxide-coated titanium was used as an electrode besides using the electrolyte of 2.5 mg L^{-1} concentration with a power density of 2.5 mA cm^{-2}. For every five mins, treated coragen samples were collected and tested for COD. Fig. 5 represents the pH of COD mineralization. When compared with other pHs such as 3, 7, and 9 (38% and 40%), it was found that the pH 5 attained the maximum COD mineralization (58%). At pH 5, the major active substance was ($HClO^-$) and at alkaline medium, the major active substance was ClO^- ions [12]. The hydroxyl radicals were produced in a better manner in acidic medium, due to the front side of Cl^- ion at a higher level in acidic medium. Earlier reports have already proved that under pHs 2, 3, and 5, the majority of the substances were hypochlorous acid (HOCl) and hypochlorite (OCl^-) ions [13]. At alkaline and neutral medium, the instability of $OH^\bullet$ causes less mineralization rate.

3.2. Various pHs on Chloride

During the electrolysis process, pH causes a chemical reaction of the oxidant in an electrolyte (NaCl). The chloride was removed at four different pH values such as 3, 5, 7, and 9. During the electrolysis, the oxidation occurs on the front side of Cl^- ions as shown (Eqs. (13)–(16)). The speciation equation for active chlorine species (Cl_2, Cl_3^-, HClO, and ClO^-) was calculated at the time of electrolysis of 2.5 mg L^{-1} NaCl for Cl^-. The Cl_3^- got produced in very low concentrations of pH 3.0, while the predominant species was Cl_2 until the pH was 5.0 whereas the HClO was in the pH range of 3–9 and it was pH > 9.0 in case of ClO^-. The mediated oxidation of coragen, with these species, was then expected to be faster in the acidic medium than alkaline medium because of the high standard potential of Cl_2 (E_0 = 1.36 V) and HClO (E_0 = 1.49) in comparison with ClO^- (E_0 = 0.89 V). Since most electrolytic processes in undivided cells occur in acidic medium, the general mineralization of pesticide is commonly referred to as follows, which remains the only chemical action of ClO^-.

$$2Cl^- + Cl(a) + 2e^- \left(\text{Standard potential of } Cl_2\right)\left(E_0 = 1.40\ \text{V}\right) \quad (13)$$

$$Cl_2 + H_2O + HOCl + H^+ + Cl^- \left(E_0 \text{ of } HOCl = 1.49\ \text{V}\right) \quad (14)$$

$$HOCl + H^+ + OCl^- \left(E_0 \text{ of } ClO^- = 0.89\ \text{V}\right) \quad (15)$$

$$\text{Coragen} + OCl^- \text{ Intermediates } CO_2 + H_2O + Cl^- \quad (16)$$

To change the pH, the equilibrium was operated in the reaction (Eq. (15)), while the HOCl substance was dominant in acidic pH. The hypochlorite ions (ClO^-) were the major substances when pH was above 9. At acidic pH, as shown in Fig. 6, the hypochlorous acid ions and chloride ions were strongly controlled by the oxidation process. The final results show that the maximum Cl_2 removal (65%) was obtained at pH 5.

3.3. Various pHs on bromide

Bromide toxicity tremendously affects human beings due to which the maximum permissible limit of bromide concentration is 25 μg L^{-1} [14–19]. Chlorotrianlipore contains bromide in its chemical structure. Heavy metals cannot be removed through oxidation due to which the current study applied *n* hap as an adsorbent to remove bromide. The bromide was observed in high quantities at pH 3 (59%). At low pH, the *n* hap surface produces huge volumes of H^+ ions. In *n* hap, the adsorbed surface becomes neutral thereby removing the hindrance to the diffusion of bromide ions. At high pH values, the reduction in adsorption is possible due to the presence of abundant OH^- ions causing increased hindrance to the diffusion of bromide ions. The efficiency of the nano-hydroxyapatite material, using different pHs, as

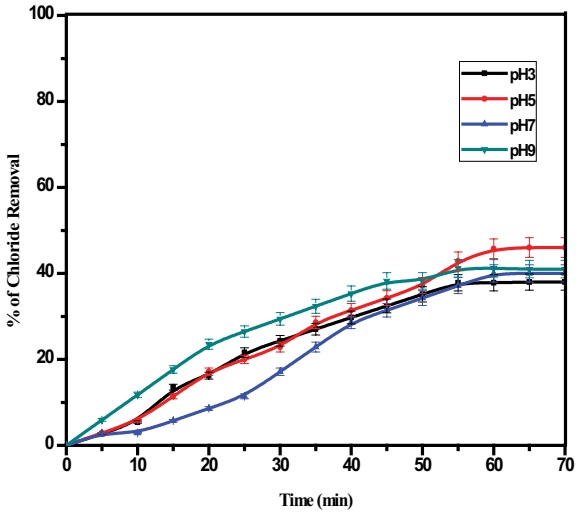

Fig. 6. Various of pH on chloride.

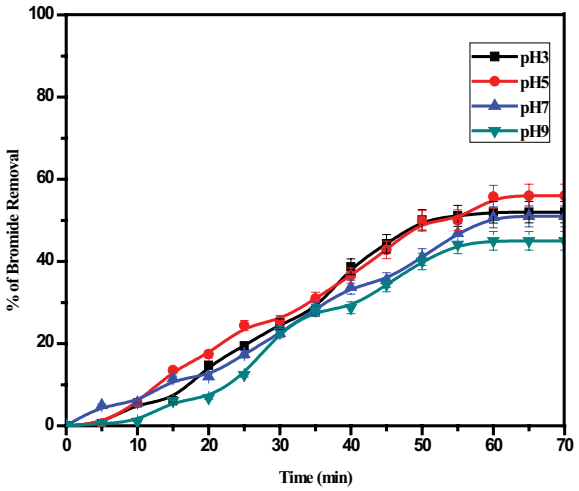

Fig. 7. Various of pH on bromide.

compared with previous studies [20–23]. The removal efficiency of heavy metal-like fluoride was very high at acidic pH [72% at pH 5, 69% at pH 3, 95% at pH 6, and 86% at pH 4]. This was because, at low pH conditions, the H^+ ions dominate the other ions. The result is shown as a graph with values plotted in Fig. 7. The bromide removal got increased at both 7 and 9 pH range because of the presence of hydroxyl ions. The OH^- hinder the diffusion of bromide ions. Fig. 7 inferred that the maximum removal of bromide was achieved at pH 3.

3.4. Various power densities on COD

The electrolysis rate is mainly controlled by power density [24–26]. To optimize the influence of power compactness on coragen removal, three different power densities were used such as 2.5, 5.0, and 7.5 mA cm^{-2} whereas 200 mg L^{-1} of coragen effluent was treated using triple oxide electrodes at various power compactness. The results obtained are shown in Fig. 8. As illustrated, when the current was increased from 2.5 to 7.5 mA cm^{-2}, the percentage of COD removal got increased to 79% for triple oxide-coated titanium anodes with *n* hap sorbent. It has been emphasized in earlier reports that the rate of mineralization increases when various power compactness' are used. In comparison with other studies, power density plays a vital role in the removal of COD. The rate of COD removal got increased when the current density was increased. Lidia et al. [35] mentioned that high power compactness, throughout the electrolysis process, increases the generation of chlorine which is mainly responsible for the removal of pollutants from coragen [27–30] (Fig. 8).

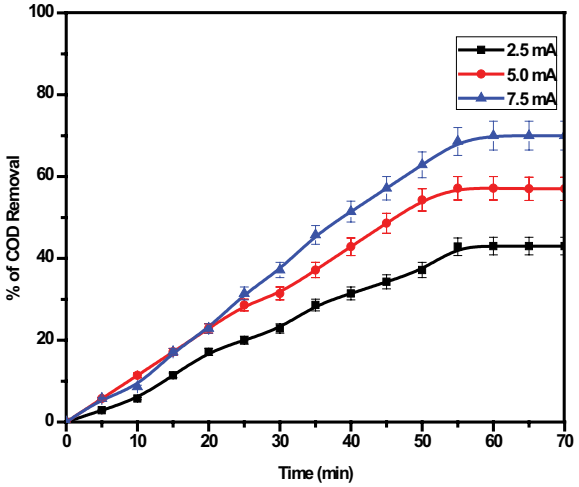

Fig. 8. Various Power density on COD.

Table 1
Some important functional groups assignments of hydroxyapatite nanoparticles

Wavenumber	Stretching mode	Functional group
3,567.70	Ion stretching group	OH^-
1,693.32	Carboxylates	CO_2
634.89	Alkyl halides	CBr
1,035.76	Polysaccharides	CO
565.70	Alkyl halides	CBr

3.5. Various power densities on chloride

Cl_2 mineralization was similar to cathodic protection where the direct power was extended into RuO_2 /IrO_2/TaO_2 coated titanium electrodes though there are two major differences noticed. The first difference is the temporary aspect of the surface anode for chloride removal which existed only during the process duration and the second difference is the higher extent power which was utilized in the removal of Cl_2 compared to cathodic protection. Power levels were decided to be practical for Cl_2 removal in the range of 2.5–7.5 mA cm^{-2}. For the removal of chloride, the same volume of power was utilized, but a minimum time period was enforced. The electrolysis processes were carried out for about 70 min under the room temperature of 25°C at pH 5 using a triple oxide-coated titanium electrode with an initial concentration of 1,000 mg L^{-1} coragen and 2.5 mg L^{-1} NaCl.

The electrode gradation was carried out at optimum power compactness of 7.5 mA cm^{-2}. At this value, there was a great possibility of an electro generation of Cl_2 in solution. At high power compactness, the production of hypochlorite ions was high. Maximum mineralization of chloride (77%) was obtained at the highest power compactness of 7.5 mA cm^{-2} within 70 min at pH 5 as shown in Fig. 9.

3.6. Various run times on COD

During coragen electrolysis, the consumption of power is an important test so that it has been conducted with different run times. The removal of chemical oxygen demand got increased with increased run time. The coragen removal got increased from 30 to 150 min impulse which was directly proportionate to the run time. The mineralization of COD was effective at the starting of electrolysis whereas the gradual value was later maintained at the end of electrolysis. The experiments were carried out for the percentage of COD removal with the operation run time of 30–150 min at constant power compactness of 2.5 mA cm^{-2} with NaCl concentration of 2.5 mg L^{-1} and constant pH 5. Fig. 10 represents the rate of COD mineralization which got increased with run time. It clearly mentioned that the coragen mineralization was directly proportional to run time.

3.7. Various run times on chloride

The wastewater run time is an essential factor for electrolysis processes. In common, larger run time increases the efficiency of electrolysis [31]. Various supporting electrolytes, on the mineralization of coragen, were examined in the presence of supporting electrolytes such as NaCl. Electrolyte concentration is one of the important factors in wastewater treatment that make use of the electrooxidation process. Previous studies proved that increasing the concentration of electrolytes favors the degradation of organic material rate [32–35]. In the current study, sodium chloride was used as an electrolyte. NaCl got split into Na^+ anion and Cl^- cation during electrolysis. The complete mineralization of coragen is primarily dependent on (Na^+) anion of the NaCl present in the effluent. The Cl^- cation got converted into chloride (Cl_2). This is the reason behind the estimation of chloride ion concentration in the current study after the electrolysis of the samples. The power compactness of 2.5 mA cm^{-2}, constant pH of 5, run time of 150 min, and the NaCl of 2.5 g concentration were maintained during the electrolysis (Fig. 11). According to the previous report published by Velstich et al. [36] a firm catalytic action of Cl_2 ion was noticed during the transition of organic pollutants to innocent carbon dioxide and water in the presence of chloride ion. According to the study published by Bhaskar Raju et al. [37] a firm catalytic action of Cl_2 ion was noticed during the transition of organic pollutants to innocent carbon dioxide and water in the presence of chloride ion.

3.8. Various run times on bromide

Various run times on the remotion of bromide using nano-hydroxyapatite were analyzed. The run time curves, given in Fig. 12, show rapid adsorption of bromide from

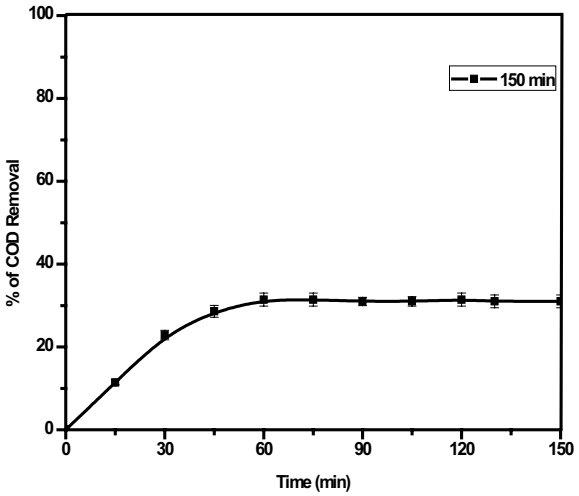

Fig. 10. Various run time on COD.

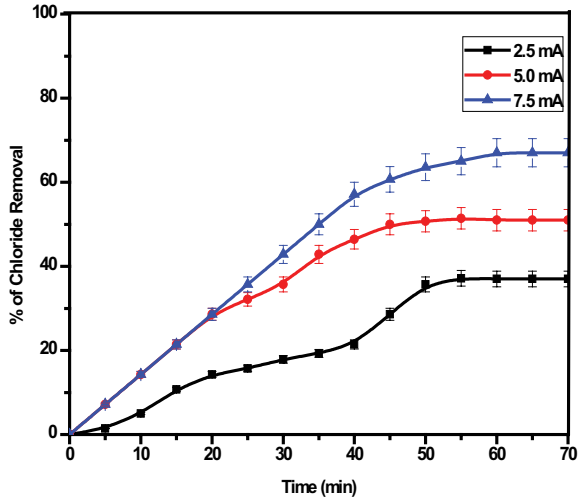

Fig. 9. Various power density on chloride.

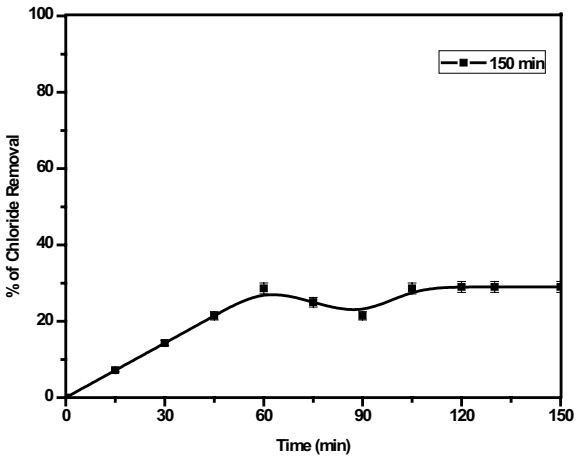

Fig. 11. Various run time on chloride.

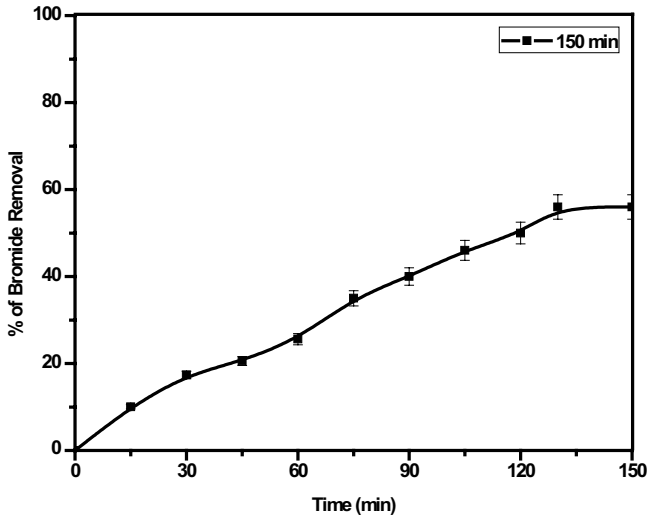

Fig. 12. Various run time on bromide.

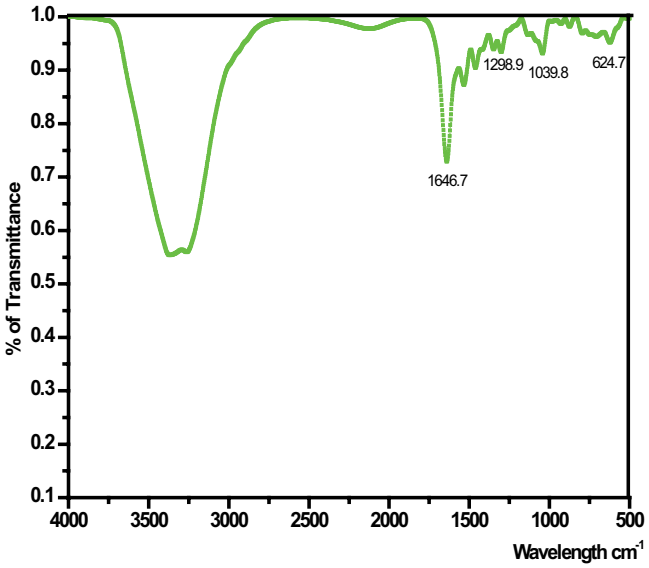

Fig. 13. FTIR image for before electrolysis of coragen.

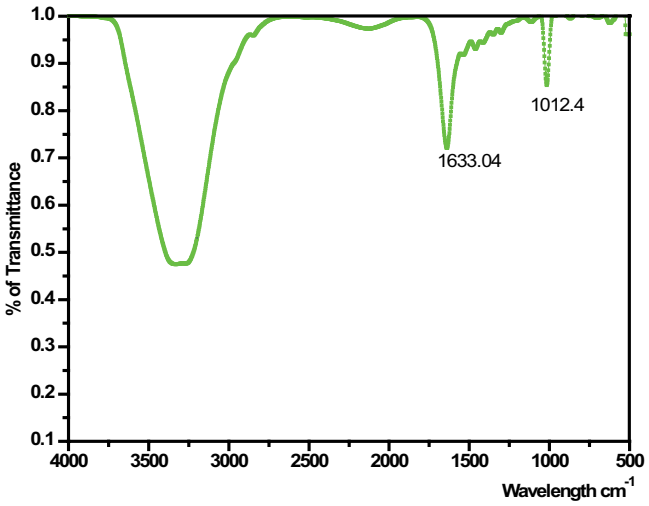

Fig. 14. FTIR image for after electrolysis of coragen.

150 min, and the bromide ions get accumulated with increased run time which makes it saturated to diffuse deeper into the adsorbent structure at the highest energy sites. This was attributed to the reason that the mesopores get filled up which resists in the diffusion of aggregated bromide molecules in the adsorbents [38]. Different run times were tested to optimize the electrolysis of coragen effluent. Five various run times were carried out for bromide removal (30, 60, 90, 120, and 150 min). At constant power compactness of 7.5 mA cm^{-2}, NaCl concentration of 2.5 mg L^{-1} and at optimum pH 3 as shown in Fig. 12, there was an increase in bromide adsorption when the run time increased. In the literature, it is proven that the increase in contact time, one can achieve high removal efficiency. Likewise, in the current study, the researcher achieved the maximum Br removal efficiency by increasing the run time. [39–41]. In the presence of *n* hap, the maximum mineralization of Br was achieved at 60 min of run time. The adsorption percentage of Br was 62% with power compactness of 7.5 mA cm^{-2} in 60 min run time. The final results represent that the bromide desorption is directly proportional to run time.

4. FTIR analysis

To determine the changes that had occurred in the functional group during electro-oxidation, the samples were monitored using FTIR spectroscopy. The experiments were conducted under optimal conditions except for the time duration which was fixed as 20 min. The 150 min treated coragen sample which had a pH of 5 with a power density of 7.5 mA cm^{-2} was used to analyze the FTIR analysis. Figs. 13 and 14 show the IR spectra of the carriage before and after the electrolysis at room temperature. The characteristic peaks of the coragen effluent (Table 1) at 3,356 cm^{-1} were due to the primary, secondary amines, and amides present in raw coragen effluent. The peaks found at 2,127; 1,640; and 1,369 cm^{-1} were mainly due to the stretching absorption of alien and carbonyls (general) groups. Besides, the peaks were obtained at 1,233; 661.05; and 597.58 cm^{-1} due to the alkyl halide C–Br stretch gojolroups respectively.

5. Gas chromatography–mass spectrometry (GC-MS) analysis

The intermediate species, formed during the mineralization of corrosion, using triple oxide-coated titanium anode were identified by GC–MS (Perkin Elmer-Clarus 600, Germany). The samples that underwent the electro-oxidation process at 5 min time intervals were collected during the electrolysis of all the samples. Through GC–MS (Perkin Elmer-Clarus 600, Germany), with MS capillary column (60 μm × 250 μm), an intermediate analysis was carried out. In this analysis, a constant flow rate of 1 mL min^{-1} helium was used as a carrier gas. The temperature of the ion source was 200°C. The initial oven temperature was maintained at 50°C for 5 min and the range of scan mode was m/z from 40 to 480 Da. The injection volume was 5 μL and under these operating conditions, the retention time for standard coragen was 17.40 min. After 60 min, the electrolysis samples were

Table 2
Comparison of different electrode potential for removal of pollutants

Electrode	Pollutants	Optimum pH	EC	% of COD removal	Reference
Triple oxide coated titanium electrode	Coragen	5	7.5 mA cm^{-2}	78.0%	In this study
Silicon-based solar cell	Organic pollutants	–	1.6 V	56.0%	Perez-Rodriguez et al. [42]
Boron doped diamond electrode	Pesticide	3.0	100 mA cm^{-2}	100.0%	Vieira Guelfi et al. [43]
Boron doped diamond electrode	Municipal wastewater	3.0	196 A m^{-2}	100.0%	Garcia-Segura et al. [44]
Boron doped diamond electrode	Lindane	3.0	400 mA	80.0%	Korbahti et al. [45]
Boron doped diamond electrode	Resorcinol	3.0	8.0 mA cm^{-2}	>86.0%	Zazoua et al. [46]
Pt	2,4,5-T	3.0	1.000 mA	>96.0%	Luo et al. [47]
Pt	Pursulfate	3.0	40.0 mA	80.0%	Luo et al. [47]
Pt	Recalcitrant indole	8.6	161 A m^{-2}	86.3%	Hiwarkar et al. [48]

analyzed for intermediates. It is necessary to discuss the role played by electrocatalyst and oxidation in the removal of COD, chloride, and bromide which are mainly attributed to the radicals and this is mainly due to electrooxidation generation of oxidant species ($OH^{\bullet}$, H_2O_2, $HOCl^{-}$, and OCl^{-} depending on the pHs). As shown in Table 2, the by-products were detected at 5 min and at pH 5 for the electrolysis process. As given in Fig. 16, after 5 min of the oxidation process, major fragments got generated in the removal process. The mineralization of the pesticide and electrolysis causes significant mineralization which results in the formation of substitutes such as (Figs. 15 and 16) (3-bromo-1-(3-chloro-2-pyridinyl)-1H-pyrazole-5-carboxylic acid, 2,6-dichloro-4-methyl-11H-pyrido [2,1-b]quinazolin-11-one,5-Bromo-N-methyl-1H-pyrazole-3-carboxamide,3-Bromo-N-[4-chloro-2hydroxymethyl)-6 [(methylamino)carbonyl] phenyl]-1-(3-chloro-2-pyridinyl)-1H-pyrazole-5carboxamide,2Amino-5-chloro-3(methylamino) carbonyl] benzoic acid, 2-[3-Bromo-1-(3-chloro-2-pyridinyl) 2–3-Nitro-1 bromide -1H-pyrazol-5-yl]-6-chloro-8-(hydroxymethyl)-4(3H)-quinazolinone, 2–3-Bromo-1-(3-chloro-2-pyridinyl), 2–3-Nitro-1 bromide and other lower molecular compounds.

6. Conclusion

The electrochemical treatment of the simulated synthetic wastewater containing pesticides (coragen) has been investigated under several operating conditions using a triple oxide-coated titanium electrode. The highest electrocatalytic activity was observed at applied power compactness of 7.5 mA cm^{-2} under optimum pH 5 and supporting NaCl of 2 mg L^{-1} concentration. The maximum removal efficiencies of coragen under optimum condition were COD, Cl, and Br 79%, 77%, and 59%. In the present investigation, it is concluded that the use of a triple oxide-coated titanium electrode and nano-hydroxyapatite (*n* hap) in the electrocatalytic

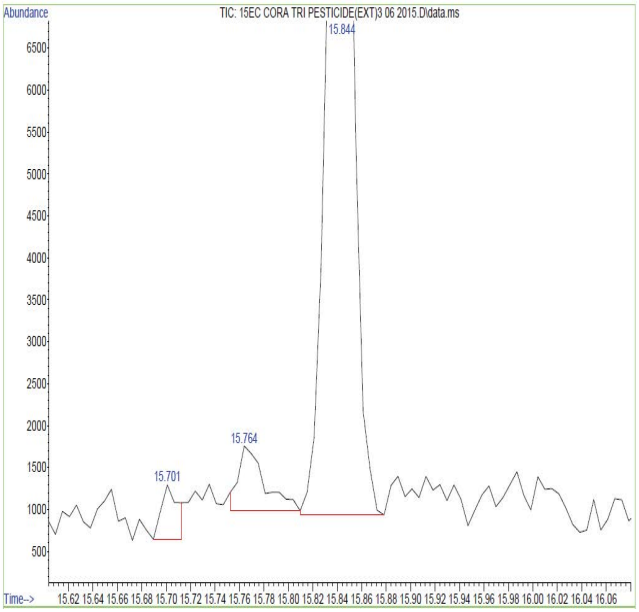

Fig. 15. GC image of coragen.

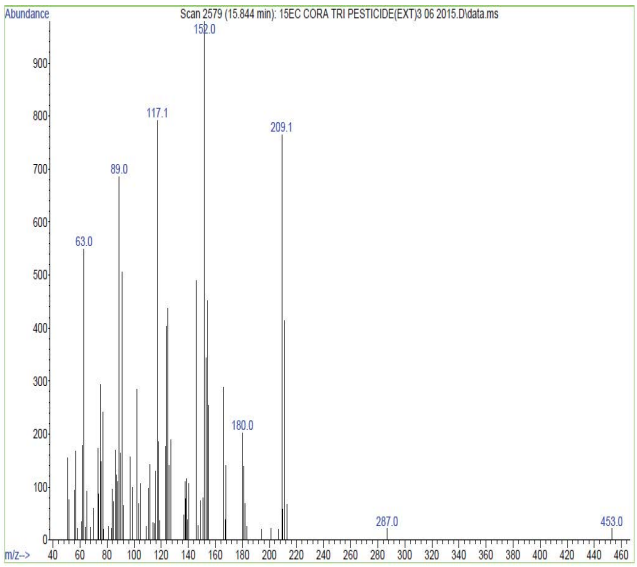

Fig. 16. MS image of coragen.

degradation played a major role. The GC–MS and FTIR results have proved that some organic compounds (coragen) led to maximum degradation. So these electrodes and *n* hap could be applied in the treatment of agricultural wastewaters that contain organic compounds such as pesticides.

References

[1] E. Vangelie, R. Campos, J. Luiz de Oliveira, L. Fernandes, Fraceto, B. Singh, Polysaccharides as safer release systems for agrochemicals, Agron. Sustainable Dev., 3 (2015) 47–66.

[2] A. Özkara, D. Akyıl, M. Konuk, Pesticides, Environmental Pollution, and Health, Elsevier, (2016), doi: 10.5772/63094.

[3] A.K. Mishra, V.K. Chandiraseharan, N. Jose, T.D. Sudarsanam, Chlorantraniliprole: an unusual insecticide poisoning in humans, Indian. J. Crit. Care. Med., 20 (2016) 742–744.

[4] J. Bartlomiej, S. Troczka Martin, M. Williamson Linda, T.G. Emyr Davies, Rapid selection for resistance to diamide insecticides in *Plutella xylostella* via specific amino acid polymorphisms in the ryanodine receptor, Neurotoxicology, 60 (2017) 224–233.

[5] Y. Liu, Y. Gao, G. Liang, L. Yanhui, Chlorantraniliprole as a candidate pesticide used in combination with the attracticides for lepidopteran moths, PLoS One, 12 (2017) 1–10, doi: org/10.1371/journal.pone.0180255.

[6] K. Dutta, M. Ali, A. Najam, R. Kumarand, A. Kumar, Ameliorative effect of seed extract of *Pterocarpus santalinus* on coragen induced haematological alterations and serum biochemical changes in charles foster rats, J. Toxicol. Environ. Health, 6 (2014) 194–202.

[7] H. Watson, Biological membranes, Essays Biochem., 59 (2015) 43–69.

[8] A. Catala, Lipid peroxidation modifies the assembly of biological membranes the lipid whisker model, Front. Physiol., 5 (2015) 1–4, doi: 10.3389/fphys.2014.00520.

[9] O. Ganzenko, D. Huguenot, E.D. Van Hullebusch, G. Esposito, M.A. Oturan, Electrochemical advanced oxidation and biological processes for wastewater treatment: a review of the combined approaches, Environ. Sci. Pollut. Res., 21 (2014) 8493–8524.

[10] Y. Feng, L. Yang, J. Liua, B.E. Logan, Electrochemical technologies for wastewater treatment and resource reclamation, Environ. Sci. Water Res. Technol., 2 (2016) 800–831.

[11] APHA, Standard Methods for the Examination for Water and Wastewater, 19th ed., American Public Health Association, Byrd Prepess Springfield, Washington DC, 1995.

[12] G. Vlyssides, D. Papaioannou, M. Loizidoy, P.K. Karlis, A.A. Zorpas, Testing an electrochemical method for treatment of textile dye wastewater, Waste Manage., 20 (2000) 569–574.

[13] Y.P. Feng, Z.H. Ni, H.M. Wang, J. Kasim, H.M. Fan, T. Yu, Y.H. Wu, Z.X. Shen, Graphene thickness determination using reflection and contrast spectroscopy, Nano Lett., 7 (2007) 27–58.

[14] G. Li, Y. Eva, Observation of landau levels of dirac fermions in graphite, Nat. Phys., 3 (2007) 623–627.

[15] D.E. Kimbrough, I.H. Suffet, Electrochemical removal of bromide and reduction of THM formation potential in drinking water, Water Res., 36 (2002) 4902–4906.

[16] M. Siddiqui, W.Y. Zhai, G. Amy, C. Mysore, Bromate ion removal by activated carbon, Water Res., 30 (1996) 1651–1660.

[17] W.J. Huang, Y.L. Cheng, Effect of characteristics of activated carbon on removal of bromated, Sep. Purif. Technol., 59 (2008) 101–107.

[18] M.J. Kirists, V.L. Snoeyink, J.C. Kruithof, The reduction of bromate by granular activated carbon, Water Res., 349 (2000) 4250–4260.

[19] M. Asami, T. Aizawa, T. Morioka, W. Nishijima, A. Tabata, Y. Magara, Bromate removal during transition from new granular activated carbon (GAC) to biological activated carbon (BAC), Water Res., 33 (1999) 2797–2804.

[20] A. Avram, T. Frentiu, O. Horovitz, A. Mocanu, F. Goga, M. Tomoaia-Cotisel, Hydroxyapatite for removal of heavy metals from wastewater, Studi a ubb chemia., 4 (2017) 93–104.

[21] F. Guzman-Duque, C. Petrier, C. Pulgarin, G. Penuela, R.A. Torres-Palma, Effects of sono chemical parameters and inorganic ions during the sono chemical degradation of crystal violet in water, Ultrason. Sonochem., 18 (2011) 440–446.

[22] N. Bishnupriya, S. Amruta, P. Rajkishore, K. Misra, Comprehensive understanding of the kinetics and mechanism of fluoride removal over a potent nanocrystalline hydroxyapatite surface, ACS Omega, 2 (2017) 8118–8128.

[23] M. Mourabet, A. El Rhilassi, H. El Boujaady, M. Bennani-Ziatni, R. El Hamri, A. Taitai, Removal of fluoride from aqueous solution by adsorption on hydroxyapatite (HAp) using response surface methodology, J. Saudi Chem. Soc., 19 (2015) 603–615.

[24] W. Aili, L. Dong, Y. Hengbo, W. Huixiong, W. Yuji, R. Min, J. Tingshun, C. Xiaonong, X. Yiqing, Size-controlled synthesis of hydroxyapatite nanorods by chemical precipitation in the presence of organic modifier, Mater. Sci. Eng., 61 (2007) 865–869.

[25] H. Zhou, F. Yu, Q. Zhu, J. Sun, F. Qin, L. Yu, J. Bao, Y.Y. Orcid, S. Chen, Z. Ren, Water splitting by electrolysis at high current densities under 1.6 V, Energy Environ. Sci., 11 (2018) 2858–2864.

[26] D. Shen, J. Ma, Y. Liu, C. Zhao, Treatment of high salinity organic wastewater by membrane electrolysis, Earth Environ. Sci., 128 (2018) 012–141.

[27] M. Muthukumar, M. Govidaraj, A. Muthusamy, G. Bhaskar Raju, Comparative study of electrocoagulation and electrooxidation processes for the degradation of ellagic acid from aqueous solution, Sep. Sci. Technol., 46 (2011) 272–282.

[28] M. Govindaraj, M. Muthukumar, G. Bhaskar Raju, Electrochemical oxidation of tannic acid contaminated wastewater by $RuO_2/IrO_2/TaO_2^-$ coated titanium and graphite anodes, Environ. Technol., 31 (2010) 1613–1622.

[29] S. Hamzah, N.I. Yatim, M. Alias, A. Ali, N. Rasit, A. Abuhabib, Extraction of hydroxyapatite from fish scales and its integration with rice husk for ammonia removal in aquaculture wastewater, Indones. J. Chem., 19 (2019) 1019–1030.

[30] A. Stefanova, S. Ayata, A. Erem, S. Ernst, H. Baltruschat, Mechanistic studies on boron-doped diamond: oxidation of small organic molecules, Electrochim. Acta., 110 (2013) 560–569.

[31] T. Ogawa, M. Takeuchi, Y. Kajikawa, Analysis of trends and emerging technologies in water electrolysis research based on a computational method: a comparison with fuel cell research, Sustainability, 10 (2018) 1–24, doi: 10.3390/su10020478.

[32] F.L. Guzman-Duque, R.E. Palma-Goyes, I. Gonzalez, G. Penuela, R.A. Torres-Palma, Relationship between anode material supporting electrolyte and current density during electrochemical degradation of organic compounds in water, J. Hazard. Mater., 278 (2014) 221–226.

[33] M. Panizza, G. Cerisola, Direct and mediated anodic oxidation of organic pollutants, Chem. Rev., 109 (2009) 6541–6569.

[34] R.E. Palma-Goyes, F.L. Guzman-Duque, G. Penuela, I. Gonzalez, J.L. Nava, R.A. Torres-Palma, Electrochemical degradation of crystal violet with BDD electrodes: effect of electrochemical parameters and identification of organic by-products, Chemosphere, 81 (2010) 26–32.

[35] S. Lidia, Claudia, N.K.A. Santosh, Comparative study on oxidation of disperse dyes by electrochemical process, ozone, hypochlorite, and Fenton reagent, Water Res., 35 (2001) 2129–2136.

[36] W. Vielstich, A. Lamn, H.A. Gasteiger, Handbook of Fuel Cells: Fundamentals, Technology and Applications, Four Volumes, John Wiley, New York, 2003.

[37] G. Bhaskar Raju, M. Thalamadai Karuppiah, S.S. Latha, S. Parvathy, S. Prabhakar, Treatment of wastewater from synthetic textile industry by electrocoagulation - electrooxidation, Chem. Eng., 144 (2008) 51–58.

[38] H. Zhang, J. Wu, Z. Wang, D. Zhang, Electrochemical oxidation of crystal violet in the presence of hydrogen peroxide, J. Chem. Technol. Biotechnol., 85 (2010) 1436–1444.

[39] S. Hsu, P.C. Singer, Removal of bromide and natural organic matter by anion exchange, Water Res., 44 (2010) 2133–2140.

[40] M. Shi, C. Guo, J. Li, J. Li, L. Zhang, X. Wang, Y. Ju, J. Zheng, X. Li, Removal of bromide from water by adsorption on nanostructured-Bi_2O_3, J. Nanosci. Nanotechnol., 17 (2017) 6951–6956.

[41] Y.-Q. Zhang, Q.-P. Wu, J.-M. Zhang, X.-H. Yang, Removal of bromide and bromate from drinking water using granular activated carbon, J. Water Health, 13 (2015) 73–78.
[42] P. Perez-Rodriguez, C. Maqueira Gonzalez, Y. Bennani, L.C. Rietveld, M. Zeman, A.H.M. Smets, Electrochemical oxidation of organic pollutants powered by a silicon-based solar cell, ACS Omega, 3 (2018) 14392–14398.
[43] D.R. Vieira Guelfi, F. Gozzi, I. Sires, E. Brillas, A. Machulek Jr., S.C. de Oliveira, Degradation of the insecticide propoxur by electrochemical advanced oxidation processes using a boron-doped diamond/air-diffusion cell, Environ. Sci. Pollut. Res., 24 (2017) 6083–6095.
[44] S. Garcia-Segura, J. Keller, E. Brillas, J. Radjenovic, Removal of organic contaminants from secondary effluents by anodic oxidation with a boron-dipped diamond anode as tertiary treatment, J. Hazard. Mater., 283 (2015) 551–557.
[45] B.K. Korbahti, P. Demirbuken, Electrochemical oxidation of resorcinol in aqueous medium using boron-doped diamond anode: reaction kinetics and process optimization with response surface methodology, Front. Chem., 5 (2017) 75–90.
[46] H. Zazoua, N. Oturan, H. Zhang, M. Hamdani, M.A. Oturan, Comparative study of electrochemical oxidation of herbicide 2,4,5-T: kinetics, parametric optimization, and mineralization pathway, Sustainable Environ. Res., 27 (2017) 15–23.
[47] H. Luo, C. Li, X. Sun, S. Chen, B.B. Ding, L. Yang, Ultraviolet assists persulfate mediated anodic oxidation of organic pollutant, J. Electroanal. Chem., 799 (2017) 393–398.
[48] A.D. Hiwarkar, S. Singh, V.C. Srivastava, C. Thakur, I.D. Mall, S.L. Lo, Electro-chemical mineralization of recalcitrant indole by platinum-coated titanium electrode: multi-response optimization, mechanistic and sludge disposal study, Int. J. Environ. Sci. Technol., 15 (2018) 349–360.